STUDY OF DEACTIVATION EFFECT OF SO_2 ON SUPPORTED $LaCoO_3$ AND $LaMnO_3$ PEROVSKITES USED AS CATALYSTS FOR TOTAL OXIDATION OF METHANE

M. Alifanti[*], **P. Grange**[**], **B. Delmon**[**]

Supported $LaCoO_3$ and $LaMnO_3$ perovskites were prepared by different synthesis procedures. Chosen carrier was $Ce_{0.8}Zr_{0.2}O_2$ solid solution. All catalysts were thoroughly characterized by S_{BET}, XRD and XPS. Catalytic activity with time-on-stream was evaluated for complete oxidation of methane in the presence of 20ppm of SO_2. The most robust catalysts were those prepared starting from citrate precursors that had increased resistance to deactivation with respect to the corresponding unsupported peroskite. Some factors responsible for perovskite deactivation in the presence of SO_2 are presented.

Introduction

Perovskites are largely used as total oxidation catalysts. This class of mixed oxides is less expensive and thermally more stable than noble metals when used for environmental purposes. However, the major limitation arises from their lower surface area thus another approach appears to be tempting, namely the deposition of the perovskites on adequate thermally stable oxides.

Gallagher et al. [1, 2] and Johnson et al. [3, 4] reported for the first time their attempts for supporting perovskites on cordierite monoliths. However, the perovskite components (mainly Co-based perovskites) usually react with the commonly used supports (alumina, silica) yielding stable compounds such as spinels, which are catalytically inactive [16-18]. For such cases a solution is the pre-coating of Al-containing support with La_2O_3 proved to be effective in preventing Co migration into the bulk of the carrier oxide [5-8].

An interesting study of Fujii et al. [9] showed that Co-based perovskites are loaded on different carrier oxides the reaction rate for propane oxidation depend in a large extent to the nature of the support. The most active catalysts were those supported on ceria and zirconia. With respect to the deposition method of perovskite on adequate supports,

---

[*] University of Bucharest, Faculty of Chemistry, Department of Chemical Technology and Catalysis, B-dul Regina Elisabeta, 4-12, 030016, Bucharest, fax: +40 21 3159249, email: m_alifanti@pcnet.ro
[**] Université Catholique de Louvain, Unité de Catalyse et Chimie des Matériaux Divisés, Croix du Sud 2, Boite 17, 1348 Louvain-la-Neuve, Belgium, fax : +32 10 473649

Analele Universității din București – Chimie, Anul XIV (serie nouă), vol. I-II, pg. 25-32

decomposition of the citrate precursors offers the possibility to obtain small particle-size perovskite-type oxides at relatively low temperatures, such as 600-700°C [10-12].

The metal loading of supported oxide catalysts is typically much higher (one or two orders of magnitude) than for noble metals due to their generally low inherent activity per exposed atom of catalysts [13-15]. An advantage for some applications, however, is that the higher overall loading of metal oxide catalyst makes them more tolerant to catalyst poisons. In the case of supported noble metal catalysts some compounds, even at low concentration, may quickly deactivate the apparently limited number of oxidation sites present [16].

In the present study were prepared $LaCoO_3$ and $LaMnO_3$ perovskites supported on $Ce_{0.8}Zr_{0.2}O_2$ (Table 1) and their robustness was evaluated in the reaction of total oxidation of methane. Several preparation methods were employed in order to see how the physico-chemical properties and the resistance to SO_2 depend on the synthesis route.

Experimental

a) Preparation of the support

The used carrier for perovskite loading was $Ce_{0.8}Zr_{0.2}O_2$. $Ce_{0.8}Zr_{0.2}O_2$ solid solution was prepared by the “citrate” method [17] and was calcined at 700°C. The calcined material was pressed at 5t/cm^2 into binderless wafers, crushed and sieved to 40-100µm particle size before perovskite deposition.

b) Preparation of supported perovskites

$La(NO_3)_3{\cdot}6H_2O$ (Aldrich), $Ce(NO_3)_3{\cdot}6H_2O$ (Fluka), $Co(NO_3)_2{\cdot}6H_2O$ (Aldrich), $Mn(NO_3)_2{\cdot}4H_2O$ (Merck) and citric acid monohydrate (Merck) were used as starting materials. Aqueous solutions with cation ratio La:M of 1:1 and La:Ce:M of 0.8:0.2:1 (M=Co, Mn) were prepared. Wet impregnation was realized following two routes:

i) by contacting the $Ce_{0.8}Zr_{0.2}O_2$ support with a solution containing the corresponding nitrates (ratio solution/solid = 10/1) in order to obtain perovskite loadings of 2, 5, 10, 15, 20 and 30%wt. The corresponding samples will be denoted as NIT-catalysts.

ii) by contacting the $Ce_{0.8}Zr_{0.2}O_2$ support with a solution of nitrates and citric acid. The amount of salts was calculated as to correspond to 2, 5, 10, 15, 20 and 30%wt perovskite on the surface of the support. The corresponding samples will be denoted as CIT-catalysts.

The obtained slurries were stirred for 5h and the water was slowly evaporated at room temperature in a revolving flask. The drying process was completed by heating the powder in a vacuum oven set at 60°C under a pressure of 200kPa for 16h.

Four samples with the nominal compositions 10%wt $LaMO_3/Ce_{0.8}Zr_{0.2}O_2$ and 20%wt $LaMO_3/Ce_{0.8}Zr_{0.2}O_2$ (M=Co, Mn) were prepared by the citrate method [17], namely mixing the corresponding nitrates with citric acid. It should be mentioned that in this case the notation $LaMO_3$ does not represent the perovskite structure but the composition. The corresponding samples will be denoted as CITRATE-catalysts.

All the samples were calcined for 5h at 700°C in air.

Two samples were prepared by mechanical mixing of appropriate amounts (10 wt% and 20 wt%, respectively) of $LaCoO_3$ previously prepared by the citrate method [17] with $Ce_{0.8}Zr_{0.2}O_2$. These oxides were calcined at 700°C before mixing. The corresponding samples will be denoted as MM-catalysts.

c) Catalyst characterization

BET specific surface areas (SSA) were determined by nitrogen adsorption on a Micromeritics ASAP 2000 instrument. Prior to each analysis the catalyst powder was degassed 2 h at 150°C under a pressure of 0.1 Pa.

XRD patterns were recorded on a Kristalloflex Siemens D5000 diffractometer using the Cu-$K\alpha$ radiation at λ=1.5418 Å. Data acquisition was realized in the 2θ range 2-65° with a scan step size of 0.03°.

XPS spectra were recorded at room temperature and under a pressure of 10^{-7} Pa on a SSX-100 Model 206 Surface Science Instrument spectrometer with monochromatized Al-$K\alpha$ radiation (hν=1486.6eV). Charge correction was made considering that the C1s signal of contaminating carbon (C-C or C-H bonds) was centered at 284.8 eV.

d) Catalytic activity evaluation

Deactivation studies were performed measuring the methane conversion (1% methane in air, 0.1 g of catalyst loaded in a U-shape quartz microreactor operating in a down-flow mode at atmospheric pressure, total flow: 75 ml/min) in isothermal conditions at 600°C in the presence of 20ppmV of SO_2. Prior to each evaluation, the catalyst was activated 2 h at 650°C under flow of air and then cooled to 600°C. The outlet and inlet gas compositions were followed using an on-line Delsi 2000 gas-chromatograph, equipped with a Carbosphere packed column and a thermal conductivity detector (TCD). Helium was used as a carrier gas at a flow of 25 ml/min and the analysis was conducted isothermally at 150°C. The intensity of deactivation can be represented by Relative Loss of Activity (RLA) defined as

$$\mathrm{RLA}=\frac{X(0)-X(15)}{X(0)}$$

where X(15) is the fractional conversion of methane after 15 hours on-stream in the presence of sulfur-dioxide and X(0) represents the initial conversion. According to the definition, the lower the value of RLA the more resistant is the catalyst.

Results and discussion

Table 1 comprises the results of textural and structural characterization of the considered catalysts. Both CIT- and NIT-samples have a lower specific surface area than $Ce_{0.8}Zr_{0.2}O_2$ support (40m²/g). The surface area decreases in parallel with the active phase loading, independent to the nature of the precursor. This shows that the materials deposited on the support block some pores for loadings larger than 2%wt. The NIT-samples present SSA systematically lower than the CIT-corresponding materials whatever the loading. XRD patterns showed either for CIT- or NIT-samples no other phases than the cubic $Ce_{0.8}Zr_{0.2}O_2$ if the loading was less than 15%wt (Table 1). Perovskite phase formation at the surface of $Ce_{0.8}Zr_{0.2}O_2$ is evidenced by XRD starting with 15%wt $LaCoO_3$.

For the NIT-sample (Table 1), apart from perovskite lines, only traces of Co_3O_4 were observed. La_2O_3 signals, indicating an incomplete perovskite formation is XRD silent showing that La^{3+} is soluble in ceria. In the case of supported $LaMnO_3$, only the perovskite peaks were observed.

The patterns of supported $La_{0.8}Ce_{0.2}MO_3$ (M=Co, Mn) were similar to the corresponding $LaMO_3$ [18]. No new lines that might be ascribed to the formation of new phases by means of a solid state reaction between La, Co or Mn with the support have been detected. In conclusion, XRD patterns showed that a pure perovskite was obtained only for impregnation with citrates, namely for CIT-catalysts.

Table 1. Specific surface area (m²/g) and phase composition of the investigated catalysts as a function of the synthesis route. Values in the parenthesis stand for bulk perovskite surface area

Catalyst	Loading (%wt)	Synthesis route			Crystallographic phases[a]		
		CIT	NIT	CITRATE	CIT	NIT	CITRATE
$LaCoO_3$ (11.3)	2	38.0	36.2	-	CZ	CZ	-
	5	30.2	27.7	-	CZ	CZ	-
	10	28.4	23.4	20.5	CZ	CZ	CZ
	15	28.2	21.7	-	CZ+P	CZ+P+Co	-
	20	25.3	19.8	18.5	CZ+P	CZ+P+Co	CZ+Co
	30	24.6	18.2	-	CZ+P	CZ+P+Co	-
$LaMnO_3$ (16.5)	5	33.2	27.2	-	CZ	CZ	-
	10	29.2	22.7	38.5	CZ	CZ	CZ
	15	27.4	19.7	-	CZ+P	CZ+P	-
	20	25.6	17.6	36.3	CZ+P	CZ+P	CZ
	30	24.2	17.8	-	CZ+P	CZ+P	-
$La_{0.8}Ce_{0.2}CoO_3$ (14.2)	10	27.3	24.4	-	CZ	CZ	-
	20	21.7	19.5	-	CZ+P	CZ+P+Co	-
$La_{0.8}Ce_{0.2}MnO_3$ (32.6)	10	32.2	21.1	-	CZ	CZ	-
	20	27.8	19.8	-	CZ+P	CZ+P	-

[a]P = perovskite phase; CZ = ceria-zirconia phase; Co – Co_3O_4 phase

Table 2 Binding energies (eV) for supported $LaCoO_3$

Loading (%wt)	La 3d5		Co 2p3		Ce 3d5		Zr 3d5	
	CIT	NIT	CIT	NIT	CIT	NIT	CIT	NIT
0	-	-	-	-	882.3	-	182.1	-
10	834.1	834.2	779.7	779.9	882.1	882.3	182.0	182.0
20	834.2	834.4	779.7	779.5	882.2	882.3	182.1	182.0
30	833.9	834.1	779.4	779.6	882.4	882.2	182.0	182.1
100	834.0	-	779.9	-	-	-	-	-

Table 3 Binding energies (eV) for supported $LaMnO_3$

Loading	La 3d5		Mn 2p3		Ce 3d5		Zr 3d5	
(%wt)	CIT	NIT	CIT	NIT	CIT	NIT	CIT	NIT
0	-	-	-	-	882.3	-	182.1	-
5	834.1	834.1	641.3	641.2	882.2	882.1	182.1	182.0
10	834.2	834.1	641.3	641.3	882.4	882.2	182.0	181.9
100	834.3	-	641.6	-	-	-	-	-

Tables 2 and 3 show some data obtained by XPS for selected catalysts. Binding energies showed that all elements are in their fully oxidized form. No significant shift of the binding energies of the elements occurred as compared to the bulk perovskites (Tables 2 and 3). Even if $LaCoO_3$ is deposited at the surface of $Ce_{0.8}Zr_{0.2}O_2$ the structure of oxygen signal remained unchanged, presenting the two characteristic peaks associated to lattice and adsorbed oxygen species (not shown).

The percent conversion of methane was used as a measure of catalytic activity.

Table 4 gives the values of Relative Loss of Activity (RLA) after 15h of isothermal combustion of methane at 600°C in the presence of 20ppm of SO_2. From the data presented, no clear-cut correlation could be seen between the loading or the nature of the phase deposited on $Ce_{0.8}Zr_{0.2}O_2$ and the resistance to SO_2. However, some observations may be made:

i) CIT-catalysts were generally more resistant than the corresponding NIT-samples;

ii) The RLA was around 0.4 for 20%wt and 30%wt loading while for loadings of 15%wt and below, the RLA was between 0.7 and 0.9. It appears that the samples with high perovskite loading had a better resistance to poisoning;

iii) mechanical mixtures and CITRATE-catalysts were the most poisoned. This is consistent with the high deactivation levels observed for bulk $LaCoO_3$, $LaMnO_3$, Co_3O_4, Mn_2O_3 [19] and $Ce_{0.8}Zr_{0.2}O_2$.

Table 4. Relative Loss of Activity (RLA) due to poisoning by SO_2

Catalyst	Loading, %wt	Relative loss of activity			
		CIT	NIT	CITRATE	MM
$LaCoO_3$	5	0.72	0.83	-	-
	10	0.75	0.41	0.75	-
	15	0.61	0.70	-	-
	20	0.38	0.61	0.87	-
	30	0.18	0.41	-	-
$LaMnO_3$	5	0.72	0.78	-	-
	10	0.66	0.71	0.82	0.79
	15	0.46	0.62	-	-
	20	0.41	0.89	0.96	0.82
	30	0.43	0.56	-	-
$La_{0.8}Ce_{0.2}CoO_3$	10	0.72	0.81	-	0.76
	20	0.34	0.88	-	0.55
$La_{0.8}Ce_{0.2}MnO_3$	10	0.52	-	-	-
	20	0.42	0.89	-	-
$Ce_{0.8}Zr_{0.2}O_2$	-	-	-	0.93	-

The tested catalysts were investigated by XRD, S_{BET} and XPS.

XRD indicated a loss of crystallinity after 15h of methane combustion in the presence of 20ppmV SO_2 at 600°C (Fig. 1). At the same time, the perovskite phase signals disappeared in parallel with Co_3O_4 formation. For Mn-containing catalysts the loss of crystallinity is accompanied by a disappearance of the perovskite signals without any new XRD detectable phase formation. These modifications are clearly caused by the SO_2 presence in the feed mixture. However, no reflection of a S-containing phase could be seen.

The used catalysts had systematically lower surface areas by about 10-20% than the fresh materials. This proved that the structural changes observed by XRD also modified the textural properties of our catalysts.

XPS measurements performed on the samples tested in the presence of SO_2 showed that the binding energy of the constitutive elements of the catalysts remained unchanged except for the case of La. The signal of $La3d_{5/2}$ had a shift from 834eV in the fresh samples (Tables 2 and 3) to 834.8-836eV (Fig. 2). The sulfur present at the surface was exclusively in the S^{6+} state (BE~169eV). According to these observations it appears that mainly lanthanum is affected, leading to superficial sulfate formation [19]. $La_2(SO_4)_3$ formation brings about the collapse of the perovskite structure by La extraction as sulfate.

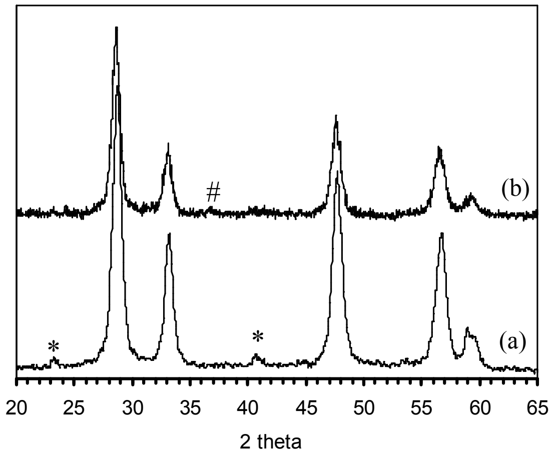

Fig. 1. *XRD patterns for CIT-20%wt $LaCoO_3$: (a) fresh sample and (b) tested in the presence of 20ppmV SO_2 at 600°C for 15h; (*) perovskite phase, (#) Co_3O_4*

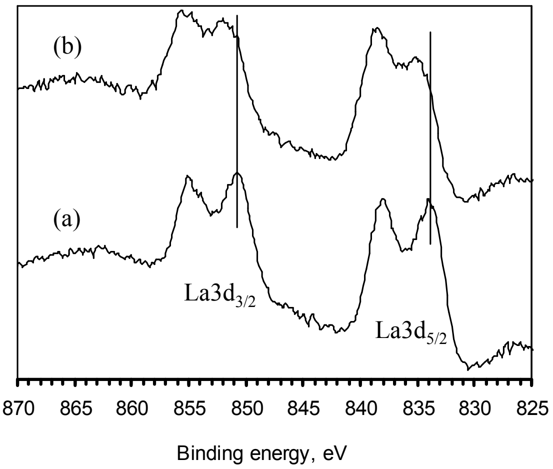

Fig. 2. *XPS signal for La3d level from a supported* $LaMnO_3$ *sample; (a) fresh catalyst and (b) tested 15h at 600°C for methane combustion (1%vol in air)in the presence of 20ppmV* SO_2

CIT-catalysts were more resistant to deactivation than the corresponding NIT-samples. This could be due to a much uniform coating of the support and, more probably, to a more homogeneous surface composition obtained by citrate decomposition [11, 18, 20]. Indeed, Co_3O_4 phase observed in XRD for fresh NIT-catalysts is the result of incomplete perovskite phase formation. For NIT-$LaMnO_3$, the parallel information provided by XRD, on which only the perovskite-phase signal is observed, and XPS, which showed surface composition different to the one of bulk $LaMnO_3$, suggest the incomplete perovskite formation and the presence of very dispersed Mn_2O_3 [18]. At the same time, it was shown that bulk Co_3O_4 and Mn_2O_3 are very active but easily poisoned by SO_2 [19]. Thus, the initial high activity that might be induced by Co or Mn oxide presence at the surface is rapidly lost.

Conclusions

A uniform dispersion of the $LaCoO_3$ and $LaMnO_3$ perovskites on $Ce_{0.8}Zr_{0.2}O_2$ support can be realized by *in situ* perovskite formation via the corresponding citrates decomposition. This facilitates the apparition of a homogeneous perovskite phase at lower temperatures than the decomposition of La, Co or Mn nitrates.

By deposition of $LaCoO_3$ and $LaMnO_3$ on $Ce_{0.8}Zr_{0.2}O_2$ the deactivation rate in the presence of SO_2 is retarded when compared to bulk perovskite. The perovskite – CeO_2 phase cooperation that was suggested in previous papers [11, 21] for explaining the abnormal resistance of $La_{1-x}Ce_xMO_3$ (x>0)(M=Co, Mn) seems to occur in the same way.

Acknowledgements

We thank the Commission of the European Union for the financial support of this research under the contract ENV4-CT97-0599.

REFERENCES

1. Gallagher, P.K., Johnson Jr., D.W., Schrey, F. (1974) *Mater. Res. Bull.* **9**, 1345
2. Gallagher, P.K., Johnson Jr., D.W., Vogel, E.M. (1977) *J. Am. Ceram. Soc.* **60**, 28
3. Johnson Jr., D.W., Gallagher, P.K., Schrey, F., Rhodes, W.W. (1976) *Am. Ceram. Soc. Bull.* **55**, 520
4. Johnson Jr., D.W., Gallagher, P.K., Schnettler, F.J., Vogel, E.M. (1977) *Am. Ceram. Soc. Bull.* **56**, 785
5. Mizuno, N., Fujii, H., Misono, M. (1986) *Chem Lett.* 1333
6. Burch, R., Harris, P.J.F., Pipe, C. (2001) *Appl. Catal. A: General* **210**, 63
7. Nudel, J.N., Umansky, B.S., Lombardo, E.A. (1987) *Appl. Catal.* **31**, 275
8. de Collongue, B., Garbowski, E., Primet, M. (1991) *J. Chem. Soc. Faraday Trans.* **87**, 2493
9. Fujii, H., Mizuno, N., Misono, M. (1987) *Chem Lett.* 2147
10. Ferri, D., Forni, L. (1998) *Appl. Catal. B : Environmental* **16**, 119
11. Kirchnerova, J., Alifanti, M., Delmon, B. (2002) *Appl. Catal. A: General* **231**, 65
12. Geus, J.W., van Giezen, J.C. (1999) *Catal. Today* **47**, 169
13. Klvana, D., Kirchnerova, J., Chaouki, J., Delval, J., Yaïci, W. (1999) *Catal. Today* **47**, 115
14. Klvana, D., Delval, J., Kirchnerova, J., Chaouki, J., (1997) *Appl. Catal. A: General* **165**, 171
15. Zhang, H.M., Teraoka, Y., Yamazoe, N. (1988) *Appl. Catal.* **41**, 137
16. Spivey, J.J., Butt, J.B. (1992) *Catal. Today* **11**, 465
17. Alifanti, M., Baps, B., Blangenois, N., Naud, J., Grange, P., Delmon, B. (2003) *Chem. Mater.* **15**, 395
18. Alifanti, M., Blangenois, N., Florea, M., Delmon, B. *Appl. Catal. A: General* (in press)
19. Alifanti, M., Auer, R., Kirchnerova, J., Thyrion, F., Grange, P., Delmon, B. (2003) *Applied Catal. B: Environmental* **41**, 71
20. Zhang, H.M., Teraoka, Y., Yamazoe, N. (1987) *Chem. Lett.* 665
21. Forni, L., Oliva, C., Vatti, F.P., Kandala, M.A., Ezerets, A.M., Vishniakov, A.V. (1996) *Appl. Catal. B: Environmental* **7**, 269